



**Fermi National Accelerator Laboratory**

**FERMILAB-Conf-95/347-E**

**CDF/D0**

## **Electroweak Results from the Tevatron**

Marcel Demarteau

*Fermi National Accelerator Laboratory  
P.O. Box 500, Batavia, Illinois 60510*

October 1995

Presented at the *XV International Conference on Physics in Collision*,  
Cracow, Poland, June 8-10, 1995

## Disclaimer

*This report was prepared as an account of work sponsored by an agency of the United States Government. Neither the United States Government nor any agency thereof, nor any of their employees, makes any warranty, expressed or implied, or assumes any legal liability or responsibility for the accuracy, completeness, or usefulness of any information, apparatus, product, or process disclosed, or represents that its use would not infringe privately owned rights. Reference herein to any specific commercial product, process, or service by trade name, trademark, manufacturer, or otherwise, does not necessarily constitute or imply its endorsement, recommendation, or favoring by the United States Government or any agency thereof. The views and opinions of authors expressed herein do not necessarily state or reflect those of the United States Government or any agency thereof.*

# Electroweak Results from the Tevatron

Marcel Demarteau  
Fermi National Accelerator Laboratory  
P.O. Box 500  
Batavia, IL 60565

Representing the CDF and DØ collaborations

## Abstract

Results from the CDF and DØ experiments are presented on properties of the  $W^\pm$  and  $Z^0$  gauge bosons using final states containing electrons and muons based on large integrated luminosities. In particular, measurements of the  $W^\pm$  and  $Z^0$  production cross sections, the  $W$ -charge asymmetry and the CDF measurement of the  $W$ -mass are summarized. Gauge boson self interactions are measured by studying di-gauge boson production and limits on anomalous gauge boson couplings are discussed.

# 1 Introduction

The CDF and DØ detectors are large multi-purpose detectors operating at the Fermilab Tevatron  $\bar{p}p$  Collider [1, 2]. The DØ detector has a non-magnetic inner tracking system, compact, hermetic uranium liquid-argon calorimetry and an extensive muon system. The CDF detector has a magnetic central detector, scintillator based calorimetry and a central muon system. During the 1992-1993 run, generally called Run 1A, the CDF and DØ experiments have collected about  $20 \text{ pb}^{-1}$  and  $15 \text{ pb}^{-1}$  of data, respectively. For the ongoing 1994-1995 run (Run 1B) both experiments have collected about  $70 \text{ pb}^{-1}$  of data. Results on the  $W$ - and  $Z$ - production cross sections, the  $W$ -width,  $W$ -charge asymmetry and the mass of the  $W$ -boson are presented. In the last section limits on possible anomalous gauge boson couplings are discussed.

## 2 IVB Production Cross Sections

In  $\bar{p}p$  collisions intermediate vector bosons are predominantly produced by quark-antiquark annihilation. In approximately 80% of the interactions a valence quark is involved. Sea-sea interactions contribute  $\approx 20\%$  of the total cross section. The leptonic decay modes of the  $W$  and  $Z$ -bosons are easily detected because of their characteristic decay signatures: a high  $p_T$  lepton accompanied by large missing transverse energy ( $\cancel{E}_T$ ) for  $W$ -decays indicating the presence of a neutrino, and two high  $p_T$  leptons for  $Z$ -decays. The measurement of the  $W$  and  $Z$  production cross sections probes the standard model of electroweak and strong interactions and provides insight in the structure of the proton. With the large increase in integrated luminosity the new measurements have a significantly improved precision. A persistent uncertainty on any cross section measurement at a  $\bar{p}p$  collider, however, is the large uncertainty on the integrated luminosity due to the uncertainty on the effective total  $\bar{p}p$  cross section seen by the detectors. This error cancels completely in the ratio of the  $W$  and  $Z$  production cross sections which can be used to extract the width of the  $W$ -boson,  $\Gamma(W)$ . The event selection is thus geared towards maximizing the cancellation of the different uncertainties in the ratio of the two cross section measurements.

The  $W$  and  $Z$  events are recorded using a common single electron trigger. The event selection for  $W$ -bosons requires an isolated lepton with transverse momentum  $p_T > 25 \text{ GeV}$  and  $\cancel{E}_T > 25 \text{ GeV}$ . Leptonic decays of  $Z$ -bosons are selected by imposing the same lepton quality cuts on one lepton, and looser requirements on the second lepton. Table 1 lists the kinematic and geometric acceptance ( $A_V$ ), trigger and event selection efficiency ( $\epsilon_V$ ) and background (Bkg) for the electron and muon decay channel for the two experiments ( $V = W$  or  $Z$ ) [3, 4, 5].

The vector boson inclusive cross section times decay branching ratio is calculated as

$$\sigma \cdot B = \frac{N_{obs} - N_{bkg}}{A \epsilon \mathcal{L}}$$

where  $N_{obs}$  is the observed number of events and  $N_{bkg}$  the calculated number of expected background events.  $B$  indicates the branching ratio of the vector boson for the decay channel under study. The measured cross sections times branching ratio are listed in table 2 and are compared with the theoretical predictions in figure 1. The theoretical predictions for the total production cross section, calculated to  $\mathcal{O}(\alpha_s^2)$  [6], depend on three input parameters: the mass of the  $W$ -boson, taken to be  $M_W = 80.23 \pm 0.18 \text{ GeV}/c^2$  [7], the mass of the  $Z$ -boson,  $M_Z = 91.19 \pm 0.004 \text{ GeV}/c^2$  [8], and the structure of the proton. Using the CTEQ2M parton distribution functions (pdf) [9], the prediction for the total cross sections are  $\sigma_W = 22.35 \text{ nb}$

	DØ		CDF	
	$e$	$\mu$	$e$	$\mu$
$W$ candidates	10338	1665	13796	6222
$A_W$ (%)	$46.0 \pm 0.6$	$24.8 \pm 0.7$	$34.2 \pm 0.8$	$16.3 \pm 0.4$
$\epsilon_W$ (%)	$70.4 \pm 1.7$	$21.9 \pm 2.6$	$72.0 \pm 1.3$	$74.2 \pm 2.7$
Bkg (%)	$5.7 \pm 0.4$	$22.1 \pm 1.9$	$12.3 \pm 1.2$	$13.1 \pm 2.0$
$\int \mathcal{L}$ (pb $^{-1}$ )	$12.8 \pm 0.7$	$11.4 \pm 0.6$	$19.6 \pm 0.7$	$18.0 \pm 0.7$
$Z$ candidates	775	77	1312	423
$A_Z$ (%)	$36.3 \pm 0.4$	$6.5 \pm 0.4$	$40.9 \pm 0.5$	$15.9 \pm 0.3$
$\epsilon_Z$ (%)	$73.6 \pm 2.4$	$52.7 \pm 4.9$	$69.6 \pm 1.7$	$74.7 \pm 2.7$
Bkg (%)	$4.0 \pm 1.4$	$10.1 \pm 3.7$	$2.1 \pm 0.7$	$0.4 \pm 0.2$
$\int \mathcal{L}$ (pb $^{-1}$ )	$12.8 \pm 0.7$	$11.4 \pm 0.6$	$19.6 \pm 0.7$	$18.0 \pm 0.7$

Table 1: Analysis results for the  $W$  and  $Z$ -production cross section measurement for CDF and DØ for the 1992-1993 data.  $A_V$ ,  $\epsilon_V$  and Bkg stand for acceptance, detection efficiency and Bkg, respectively, for vector boson  $V$ .

and  $\sigma_Z = 6.708$  nb. Using the leptonic branching ratio  $B(W \rightarrow \ell\nu) = (10.84 \pm 0.02)\%$ , as calculated following reference [10] using the above quoted  $W$ -mass, and  $B(Z \rightarrow \ell\ell) = (3.367 \pm 0.006)\%$  as measured by the LEP experiments [8], the theoretical predictions for the total inclusive production cross section times branching ratio are  $\sigma_W \cdot B(W \rightarrow \ell\nu) = 2.42_{-0.11}^{+0.13}$  and  $\sigma_W \cdot B(Z \rightarrow \ell\ell) = 0.226_{-0.009}^{+0.011}$ . The two largest uncertainties on the theoretical prediction are the choice of parton distribution function (4.5%) and the uncertainty due to using a NLO parton distribution function with a full  $\mathcal{O}(\alpha_s^2)$  theoretical calculation (3%). The experimental error is dominated by the uncertainty on the luminosity.

The ratio of the cross section measurements, in which the error on the luminosity cancels completely, measures the leptonic branching ratio of the  $W$ -boson. It can be used, within the framework of the standard model, to extract the total width of the  $W$ -boson:

$$R = \frac{\sigma_W \cdot B(W \rightarrow \ell\nu)}{\sigma_Z \cdot B(Z \rightarrow \ell\ell)} = \frac{\sigma_W}{\sigma_Z} \cdot \frac{\Gamma(W \rightarrow \ell\nu)}{\Gamma(Z \rightarrow \ell\ell)} \frac{\Gamma(Z)}{\Gamma(W)}$$

which gives

$$B^{-1}(W \rightarrow \ell\nu) = \frac{\sigma_W}{\sigma_Z} \cdot \frac{1}{B(Z \rightarrow \ell\ell)} \cdot \frac{1}{R}$$

Using the standard model prediction [10] for the partial decay width  $\Gamma(W \rightarrow \ell\nu)$  the total width  $\Gamma_W$  is given by

$$\Gamma_W = \frac{\sigma_W}{\sigma_Z} \cdot \frac{\Gamma(W \rightarrow \ell\nu)}{B(Z \rightarrow \ell\ell)} \cdot \frac{1}{R}$$

The ratio of the cross sections, using again the calculation of [6], is determined to be  $3.33 \pm 0.03$ . The error is again dominated by the choice of parton distribution functions. Note that in the ratio, also the theoretical uncertainties largely cancel. Using, as before, the measured branching ratio  $B(Z \rightarrow \ell\ell) = (3.367 \pm 0.006)\%$  and the theoretical prediction for the partial decay width  $\Gamma(W \rightarrow \ell\nu) = 225.2 \pm 1.5$  MeV [7, 10] the branching ratio, as determined from the combined DØ

	$\sigma_W \cdot B(W \rightarrow \ell\nu)$	$\sigma_Z \cdot B(Z \rightarrow \ell\ell)$
1992-1993		
DØ (e)	$2.36 \pm 0.02 \pm 0.15$	$0.218 \pm 0.008 \pm 0.014$
DØ ( $\mu$ )	$2.09 \pm 0.06 \pm 0.25$	$0.178 \pm 0.022 \pm 0.023$
CDF (e)	$2.49 \pm 0.12$	$0.231 \pm 0.012$
CDF ( $\mu$ )	$2.48 \pm 0.031 \pm 0.16$	$0.203 \pm 0.010 \pm 0.012$
1994-1995		
DØ (e)	$2.24 \pm 0.02 \pm 0.20$	$0.226 \pm 0.006 \pm 0.021$
DØ ( $\mu$ )	$1.93 \pm 0.04 \pm 0.20$	$0.159 \pm 0.014 \pm 0.022$

Table 2: Measured cross section times branching ratio for  $W$  and  $Z$  production based on integrated luminosities of 12.8 (11.4)  $\text{pb}^{-1}$  and 19.6 (18.0)  $\text{pb}^{-1}$  for the electron (muon) channel for DØ and CDF, respectively for the 1992-1993 data and the preliminary DØ results for 25.1 (30.7)  $\text{pb}^{-1}$  for the 1994-1995 data.

electron and muon 1992-1993 data, is  $(11.02 \pm 0.5)\%$ ; the CDF measured branching ratio, based on the 1992-1993 electron data is  $(10.94 \pm 0.33 \pm 0.31)\%$ . Using the calculated partial leptonic branching ratio, these measurements yield for the width  $\Gamma_W = 2.044 \pm 0.093 \text{ GeV}$  [5] and  $\Gamma_W = 2.043 \pm 0.082 \text{ GeV}$  [3], respectively. The CDF value differs from their published value due to the use of more recent experimental measurements in evaluating the input parameters. Figure 2 shows the world measured  $W$ -width values together with the theoretical prediction [3, 5, 11, 12].

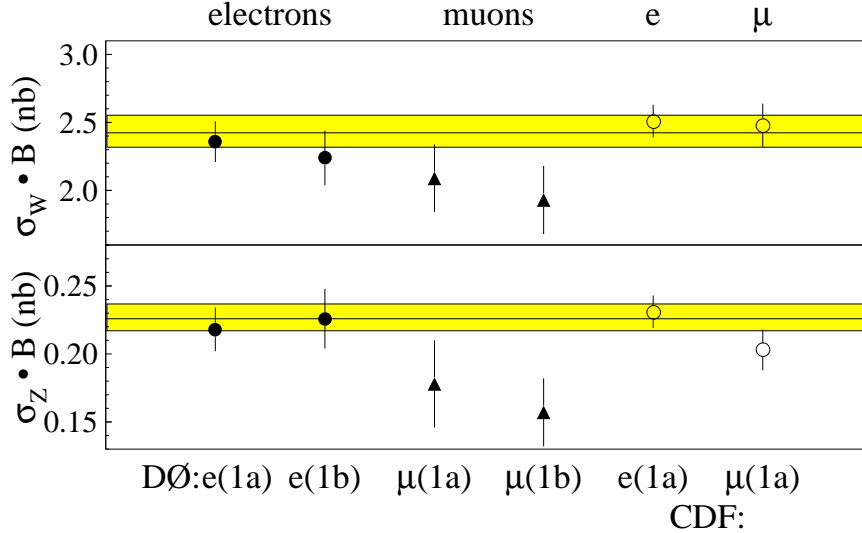


Figure 1: Measurements of the  $W$  and  $Z$  inclusive cross section compared to the theoretical predictions using the CTEQ2M parton distribution function. The shaded bands indicate the uncertainty on the predictions.

Taking into account that the ratio of the total cross sections  $\sigma_W/\sigma_Z$  is slightly different at a center of mass energy of 630 GeV ( $\sigma_W/\sigma_Z(\sqrt{s} = 630 \text{ GeV}) = 3.26 \pm 0.09$ ), and accounting for the correlation between the measurements at different center of mass energies through the choice of parton distribution functions, the different values of  $\Gamma_W$  can be combined to give a

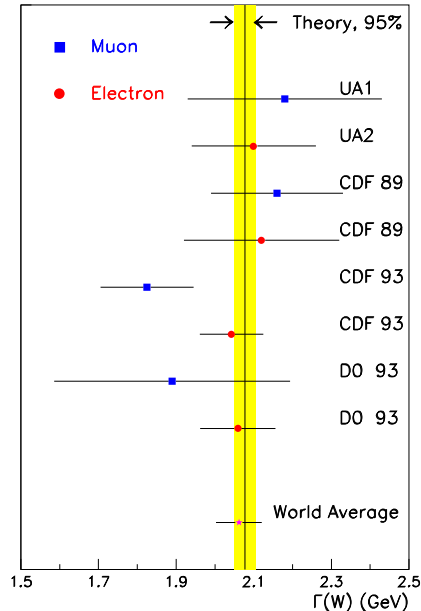


Figure 2: Measurements of  $\Gamma_W$  compared with the standard model expectation.

world average of  $\Gamma_W = 2.062 \pm 0.059$  GeV, a measurement at the 3% level. This is in good agreement with the standard model prediction of  $\Gamma(W) = 2.077 \pm 0.014$  GeV. The comparison of the measurement with the theoretical prediction can be used to set an upper limit on an “excess width”  $\Delta\Gamma_W \equiv \Gamma_W(\text{meas}) - \Gamma_W(\text{SM})$ , allowed by experiment for non-standard model decay processes, such as decays into supersymmetric particles or into heavy quarks. Comparing the above world average value of  $\Gamma_W$  with the standard model prediction a 95% C.L. upper limit of  $\Delta\Gamma < 109$  MeV on unexpected decays can be set.

Since the intermediate vector bosons are produced through a Breit-Wigner resonance the lineshape of the mass distribution contains information about the width of the boson [13]. For  $W$ -bosons, the high tail of the transverse mass distribution, where the Breit-Wigner shape dominates over the detector resolutions, can be used to extract  $\Gamma_W$ . Using a binned log-likelihood method, CDF has fit the transverse mass\* ( $m_T$ ) distribution far above the  $W$  pole ( $m_T > 110$  GeV/ $c^2$ ) to Monte Carlo generated templates with varying  $W$ -width [14]. Using this method the  $W$ -width has been determined to be  $\Gamma_W = 2.11 \pm 0.28 \pm 0.16$  GeV, where the systematic error (8%) is dominated by uncertainties in modelling the  $W$  transverse momentum distribution (6%) and the  $E_T$  resolution (5%). Although the precision of this method is currently not competitive with the extraction of the width from the ratio of cross sections, it has the advantage that it is relatively independent of standard model assumptions.

\*Transverse mass is defined as the invariant mass of the lepton and the neutrino of the  $W$ -decay in the transverse plane, see section 4.

### 3 $W$ -charge Asymmetry

The uncertainty in the structure of the proton is one of the largest errors in the theoretical prediction of the total vector boson production cross section. It also affects the uncertainties on other measurements, like the measurement of the  $W$ -mass and the cross section of di-boson production. Fortunately, the structure of the proton can be constrained at the appropriate  $Q^2$ -scale by measuring the charge asymmetry in  $W$ -production itself. The two sources that contribute to the  $W$ -charge asymmetry are the production and decay processes. Since on average a  $u$ -quark carries more momentum than a  $d$ -quark, more  $W^+$ -bosons are produced along the proton direction than along the anti-proton direction resulting in a production charge asymmetry defined as

$$A(y_W) = \frac{dN^+(y_W)/dy - dN^-(y_W)/dy}{dN^+(y_W)/dy + dN^-(y_W)/dy} \propto \frac{d(x_2)/u(x_2) - d(x_1)/u(x_1)}{d(x_2)/u(x_2) + d(x_1)/u(x_1)} \quad (1)$$

where  $x_1$  ( $x_2$ ) is the momentum fraction carried by the parton in the proton (antiproton). The  $W$ -rapidity  $y_W$ , however, cannot unambiguously be reconstructed because of the two-fold ambiguity in the longitudinal momentum of the neutrino. The quantity that is measured experimentally is the decay lepton charge asymmetry, defined as

$$A(y_\ell) = \frac{dN^+(y_\ell)/dy_\ell - dN^-(y_\ell)/dy_\ell}{dN^+(y_\ell)/dy_\ell + dN^-(y_\ell)/dy_\ell}$$

where  $N^{+(-)}$  is the number of positively (negatively) charged leptons detected at pseudorapidity  $y_\ell$ . Since the rapidity of the decay leptons is measured there is an additional contribution from the  $V-A$  coupling of the  $W$ , which partially undoes the production asymmetry. Since  $W$ -bosons are produced through  $ud$ -quark annihilation they are almost fully polarized and the lepton from, for example, the  $W^+$ -decay is preferentially emitted along the anti-proton direction. Because of  $\mathcal{CP}$  symmetry  $A(+y) = -A(-y)$  and the measured asymmetries at positive and negative rapidities can be combined.

Since the  $V-A$  structure of the  $W$ -decay is very well understood, the charge asymmetry measurement probes the structure of the proton in the  $x$  range 0.007 to 0.27. In particular, the measurement is sensitive to the slope of the ratio of the  $u$  and  $d$  parton distribution functions (cf. eq. (1)).

The CDF experiment, based on an integrated luminosity of about 20 pb<sup>-1</sup> measured the charge asymmetry for  $W$ -decays into electrons and muons and significantly constrained the then current parton distribution functions [15]. For this analysis the lepton transverse momentum,  $p_T^\ell$ , and the missing transverse momentum,  $\cancel{p}_T$ , were both required to be greater than 25 GeV/c. The leptons were detected in a pseudorapidity range  $|\eta| < 1.0$  and  $|\eta| < 2.4$  for muons and electrons, respectively. Since the measurement is a ratio measurement, many systematic errors cancel and the total systematic error is about 20% of the statistical error. Figure 3a shows the measured asymmetry for electrons and muons as a function of the lepton rapidity together with the theoretical prediction for different parton distribution functions. The predictions were obtained using the DYRAD NLO Monte Carlo [16].

Since the asymmetry measurement was not included in the determination of any of these parton distribution functions it provides an independent discriminator. The disagreement between theory and experiment can be quantified by defining the significance of the disagreement

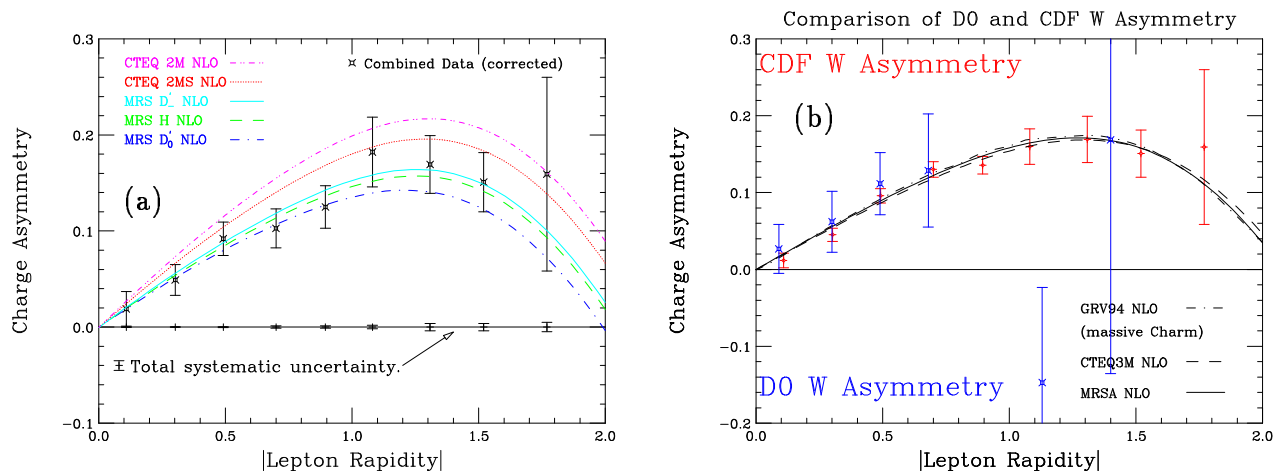


Figure 3: (a) CDF run 1a measured lepton charge asymmetry compared to NLO predictions for different parton distribution functions. The error bars are the total errors. The systematic errors are indicated on the null-asymmetry line. (b) Preliminary run 1a and run 1b CDF (o) and D0 (x) measured lepton charge asymmetry compared to NLO predictions for recent parton distribution functions.

between the weighted mean asymmetry ( $\bar{A}$ ) from theory and experiment as

$$\zeta = \frac{\bar{A}_{pdf} - \bar{A}_{data}}{\sigma(\bar{A}_{data})} \quad (2)$$

Here  $\bar{A}_{data}$  is determined over the range  $0.2 < |\eta| < 1.7$  with corresponding error  $\sigma(\bar{A}_{data})$ . The measurement clearly favors the MRS [17] parton distribution functions over the CTEQ2 [9] distributions. This constraint on the parton distribution functions can then be used to limit the error on the  $W$ -mass measurement, as will be discussed in the next section.

Figure 3b shows the updated CDF charge asymmetry, including the preliminary run 1b data, based on an integrated luminosity of  $50 \text{ pb}^{-1}$ , together with the D0 measurement. Because the D0 experiment has an outer toroidal magnetic field, the measurement is based on muons only. To minimize any detector induced bias, equal amounts of data are taken with reversed magnet polarity. The D0 measurements have a larger pseudorapidity coverage, but still suffer from smaller statistics. The three theoretical predictions are based on the MRSA [18], CTEQ3M [9] and GRV94 [19] parton distribution functions, all of which include the published CDF asymmetry measurement shown in figure 3a in the structure function determination. There is obviously an excellent agreement between the data and the theory and between the CDF and D0 measurements.

## 4 $W$ -mass

The mass of the  $W$ -boson is one of the fundamental parameters of the standard model. A precision measurement of the  $W$ -boson mass allows for a stringent test of the radiative corrections in the standard model. Combined with the measurement of the mass of the top-quark and precision measurements from  $e^+e^-$  and neutrino scattering experiments, inconsistencies

between the different measurements and the theoretical predictions can be looked for, possibly indicating processes beyond the standard model. In the following, the measurement of the  $W$ -mass by the CDF experiment will be described [20].

In essence, only two quantities are measured in  $W$ -events, namely the lepton momentum and the transverse momentum of the recoil system. The latter consists of the “hard”  $W$ -recoil and the underlying event contribution, which for  $W$ -events are inseparable. The transverse momentum of the neutrino is inferred from these two observables. Since the longitudinal momentum of the neutrino cannot be determined unambiguously, the  $W$ -boson mass is determined using the transverse mass:

$$m_T = \sqrt{2 p_T^e p_T^\nu (1 - \cos \varphi^{e\nu})}$$

where  $\varphi^{e\nu}$  is the angle between the electron and neutrino in the transverse plane. Since there is no analytical description of the transverse mass distribution, the  $W$ -mass is determined by fitting Monte Carlo generated templates in transverse mass for different masses of the  $W$ -boson to the data distribution. The quantity transverse mass is preferred over the lepton transverse momentum spectra because it is, to first order, independent of the transverse momentum of the  $W$ .

The determination of the momentum and energy scale for the leptons, and the detector response to the recoil system is crucial for the  $W$ -mass determination. For the CDF experiment, the momentum scale of the central magnetic tracker is set by scaling the measured  $J/\Psi$ -mass to the world average value using  $J/\Psi \rightarrow \mu^+ \mu^-$  decays. Based on a sample of approximately 60,000 events a scale factor of  $0.99984 \pm 0.00052$  has been derived. The dominant contribution to the error comes from the uncertainty in the amount of material the muons traverse. This procedure establishes the momentum scale at the  $J/\Psi$ -mass, where the average muon  $p_T$  is about 3 GeV/c, and needs to be extrapolated to the momentum range appropriate for leptons from  $W$ -decays. The error due to possible nonlinearities in the momentum scale is addressed by studying the measured  $J/\Psi$ -mass as function of  $\langle 1/p_T^2 \rangle$ , extrapolated to zero curvature. This extrapolation, which includes an uncertainty on a possible non-linearity of the momentum measurement, increases the error on the momentum scale to 0.00058 at the  $W$ -mass. This results in an error on the  $W$ -mass of 50 MeV/c<sup>2</sup>.

Having established the momentum scale, the calorimeter energy scale is determined from a lineshape comparison of the observed  $E/p$  distribution with a detailed Monte Carlo prediction as shown in figure 4. A two-dimensional fit of Monte Carlo generated  $E/p$  distributions in the energy scale and the electron momentum resolution is used to establish the absolute calorimeter energy scale. The scale factor is extracted from a fit over the range  $0.9 < E/p < 1.1$ . Since the momentum measurement is very sensitive to bremsstrahlung effects, the energy scale determination is critically dependent on an accurate modelling of the amount of material the electrons traverse. Using the ratio of events in the region  $1.3 < E/p < 2.0$  to the events in the range  $0.8 < E/p < 1.2$  the amount of material is determined to be  $(8.9 \pm 0.9)\% X_0$ , consistent with independent checks using photon conversions and  $Z$ -events but slightly higher than from a direct accounting of the material. The limited statistics in the high  $E/p$  region is the dominant source of the systematic error on the amount of material traversed by electrons and thus on the energy scale determination. The uncertainty of 10% on the amount of material in front of the calorimeter contributes a 70 MeV/c<sup>2</sup> uncertainty on the  $W$ -mass. The other two main contributions to the total energy scale error is a 65 MeV/c<sup>2</sup> error due to the statistics in the  $E/p$ -peak and a 50 MeV/c<sup>2</sup> error from the uncertainty on the electron resolution. The total error on the  $W$ -mass from setting the energy scale using the momentum scale is thus

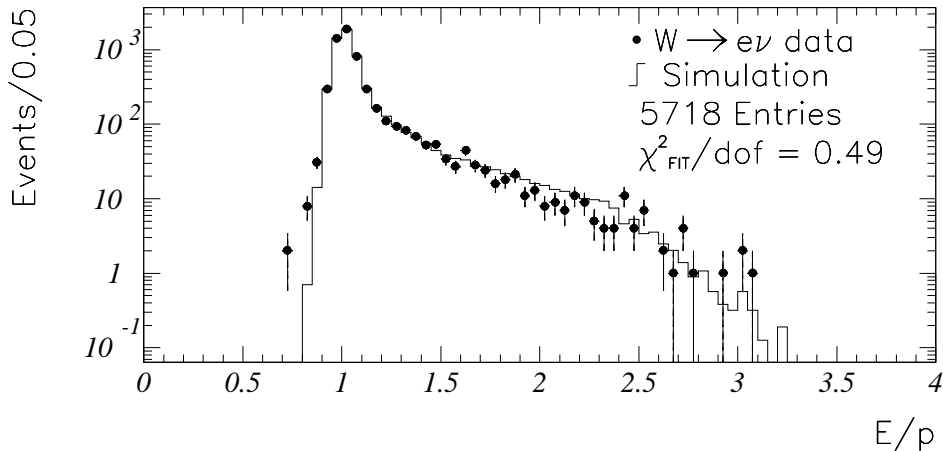


Figure 4: The  $E/p$  distribution for electrons in the  $W$ -sample (points) with the best fit from the simulation (histogram).

110 MeV/c<sup>2</sup> which, combined with the 50 MeV/c<sup>2</sup> momentum scale uncertainty, gives a total energy scale uncertainty on the  $W$ -mass of 120 MeV/c<sup>2</sup>.

The energy and momentum scales are verified by measuring the masses of known resonances, like the  $Z$ -mass and the masses of the  $\Upsilon$  resonances. They are all in good agreement with the world average values. The width of the  $Z$ -resonance provides a constraint on the momentum resolution that results in a systematic error on the  $W$ -mass from the uncertainty on the momentum and energy resolution of 60 MeV/c<sup>2</sup> and 80 MeV/c<sup>2</sup> for the muon and electron measurement, respectively. The hadronic energy scale does not need to be determined separately since  $Z \rightarrow e^+e^-$  collider events are used to model the  $W$ -recoil system.

The  $W$ -mass is determined from a maximum likelihood fit of Monte Carlo generated templates in transverse mass to the data distribution. In the Monte Carlo model of  $W$ -production, events are generated according to a relativistic Breit-Wigner resonance, with a longitudinal momentum distribution as given by the chosen parton distribution function. The nominal parton distribution function is the MRSD'- pdf. The transverse momentum of the  $W$  is then generated according to the measured  $p_T$  distribution of  $Z$ -events. This procedure can be justified because of the similarity between  $W$  and  $Z$ -production and because there are large uncertainties, both theoretical as well as experimental, on the  $W$   $p_T$ -distribution. This procedure has an added advantage that the recoil system does not need to be modeled independently, since it is taken directly from  $Z$ -events with the two leptons removed. This recoil distribution from  $Z$ -events is corrected for the lepton removal and modified to match the width of the distribution of the projection of the  $p_T$  of the recoil system perpendicular to the electron direction in data and Monte Carlo. The disadvantage of the method is that very few events (555 events to be precise) are used to model the recoil with a slightly different acceptance than for  $W$ -events and it ignores the correlation between the transverse and longitudinal momenta and the difference in mass between the  $W$  and  $Z$ -boson.

To avoid any detector biases, very tight fiducial cuts are applied in the selection of the data sample. For the electron and the muon data samples, only central leptons are selected

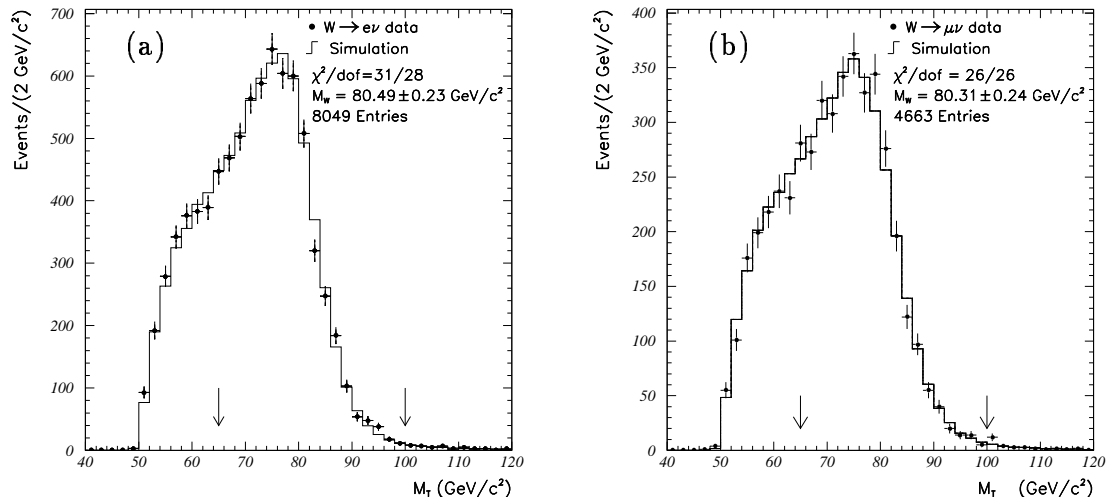


Figure 5: Transverse mass distribution of (a)  $W \rightarrow e\nu$  and (b)  $W \rightarrow \mu\nu$  decays. The points are the data and the histogram is the best fit to the data. The arrows indicate the range used to extract the  $W$ -mass.

( $|\eta| < 1$ ) with  $E_T^\ell > 25$  GeV and  $\cancel{E}_T > 25$  GeV. In addition no jets with  $E_T > 30$  GeV should be present in the event. Events with tracks with  $p_T > 10$  GeV/c in an isolation cone around the lepton are excluded and the total transverse momentum of the  $W$ ,  $p_T^W$ , is required to be less than 20 GeV/c. This event selection yields 8049 and 4663 events for electron and muon decays of the  $W$ , respectively. The mass of the  $W$  is obtained from a fit over  $65 < m_T < 100$  GeV/c<sup>2</sup>. Figure 5 shows the transverse mass distribution for the data together with the best fit of the Monte Carlo for the muon and electron channel. The  $W$ -mass is determined to be  $M_W^\mu = 80.310 \pm 0.205(stat) \pm 0.130(sys)$  GeV/c<sup>2</sup> based on 3268  $W \rightarrow \mu\nu$  events in the mass fitting window and  $M_W^e = 80.490 \pm 0.145(stat) \pm 0.175(sys)$  GeV/c<sup>2</sup> based on 5718 events.

Source	e	$\mu$	common
Statistical	145	205	—
Energy scale	120	50	50
$E$ or $p$ resolution	80	60	—
$p_T^W$ and recoil model	75	75	65
pdf's	50	50	50
QCD/QED corr's	30	30	30
$W$ -width	20	20	20
Backgrounds/bias	30	40	5
Fitting procedure	10	10	—
Total	230	240	100
Combined	180		

Table 3: Errors on  $M_W$

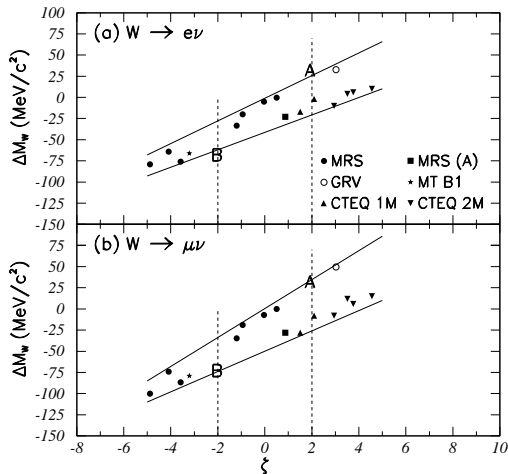


Figure 6: Correlation between  $\Delta M_W$  and  $\zeta$ , the significance of the difference between data and theory for the  $W$ -charge asymmetry, for various parton distribution functions for the  $W \rightarrow e\nu$ - and  $W \rightarrow \mu\nu$ -sample, where  $\Delta M_W = M_W^{\text{pdf}} - M_W^{\text{MRS D}'-}$ .

Table 3 lists the systematic errors on the individual measurements and the common errors. Of the errors not discussed so far, the error due to the  $p_T^W$  and recoil model and the proton structure are the dominant ones. The error due to the parton distribution inside the proton is constrained by the  $W$ -asymmetry measurement. Figure 6 shows the correlation between  $\Delta M_W$  and the significance of the deviation of the theoretical prediction and the data for the  $W$ -asymmetry for the electron and muon channel separately (cf. eq. (2)). The error on  $M_W$  is the symmetrized spread in masses for  $-2 < \zeta < 2$ . The error from the recoil model is mainly due to the statistical fluctuations arising from the finite size of the  $Z \rightarrow e^+e^-$  sample and is evaluated by Monte Carlo simulation. Skewing the  $p_T^W$ -spectrum, the error from the uncertainty of the input  $p_T^W$ -spectrum is determined. The total error from the  $p_T^W$  and recoil model is  $75 \text{ MeV}/c^2$ .

## 5 Gauge Boson Pair Production

Gauge boson self-interactions are the direct consequence of the non-Abelian  $SU(2) \times U(1)$  gauge symmetry. A direct measurement of the self-interactions, possible through the study of di-gauge boson production, is one of the remaining crucial tests of the standard model. Deviations from standard model predictions could signal new physics. The cross sections for di-boson production, however, are all extremely small. For example, the predicted cross section for  $W$ -pair production with  $WW \rightarrow \ell\nu\nu$  ( $\ell = e, \mu$ ) is about  $0.5 \text{ pb}$  and large integrated luminosities would be needed for a significant measurement of the gauge couplings. The standard model process of  $W$ -pair production, however, is characterized by large cancellations between the  $s$  and  $t$  channel production processes. The contributions from the  $t$  channel diagrams by themselves would violate unitarity. This implies that if the couplings deviate from their standard model values the gauge cancellations are destroyed and a large increase of the cross section is observed.

Moreover, the differential distributions will be modified giving rise to gauge bosons with a large transverse boost since the largest gauge cancellations occur for highly boosted gauge bosons.

The vertex of interest for the study of gauge boson self couplings is the coupling of a photon or  $Z$ -boson to a pair of  $W$ -bosons. For  $\bar{p}p$  interactions the sensitivity to the self interactions is, to first order, only through  $s$ -channel interactions. The most general effective Lagrangian, invariant under  $U(1)_{EM}$ , for the electroweak gauge interactions contains eight independent coupling parameters, the  $\mathcal{CP}$ -conserving parameters  $\kappa_V$  and  $\lambda_V$  and the  $\mathcal{CP}$ -violating parameters  $\tilde{\kappa}_V$  and  $\tilde{\lambda}_V$ , where  $V = \gamma$  or  $Z$ . The  $\mathcal{CP}$ -conserving parameters are related to the magnetic dipole ( $\mu_W$ ) and electric quadrupole ( $Q_W^e$ ) moments of the  $W$  boson, while the  $\mathcal{CP}$ -violating parameters are related to the electric dipole ( $d_W$ ) and the magnetic quadrupole ( $Q_W^m$ ) moments:  $\mu_W = (e/2m_W)(1 + \kappa_\gamma + \lambda_\gamma)$ ,  $Q_W^e = (-e/m_W^2)(\kappa_\gamma - \lambda_\gamma)$ ,  $d_W = (e/2m_W)(\tilde{\kappa}_\gamma + \tilde{\lambda}_\gamma)$ ,  $Q_W^m = (-e/m_W^2)(\tilde{\kappa}_\gamma - \tilde{\lambda}_\gamma)$  [21].

In the standard model the couplings at tree level are uniquely determined by the  $SU(2) \times U(1)$  gauge symmetry:  $\kappa_V = 1$  ( $\Delta\kappa_V = \kappa_V - 1 = 0$ ),  $\lambda_V = \tilde{\kappa}_V = \tilde{\lambda}_V = 0$ . Because of the similarity of the  $\mathcal{CP}$ -conserving and  $\mathcal{CP}$ -violating terms in the Lagrangian, the kinematic behavior of these terms is similar and the limits on both sets of anomalous couplings will be approximately the same. Therefore  $\mathcal{CP}$ -violating terms will not be discussed explicitly. Also, unless stated, it will be assumed that  $\Delta\kappa_\gamma = \Delta\kappa_Z$  and  $\lambda_\gamma = \lambda_Z$ .

A  $WWV$  interaction Lagrangian with constant, anomalous couplings violates unitarity at high energies and therefore the coupling parameters must be modified [22] to include form factors, that is,  $\Delta\kappa(\hat{s}) = \Delta\kappa/(1 + \hat{s}/\Lambda^2)^2$  and  $\lambda(\hat{s}) = \lambda/(1 + \hat{s}/\Lambda^2)^2$ , where  $\hat{s}$  is the square of the center of mass energy of the subprocess.  $\Lambda$  is a form factor scale to avoid violating unitarity.

The  $ZZ\gamma$  and  $Z\gamma\gamma$  trilinear gauge boson couplings are described in a way analogous to the  $WWV$  couplings. The most general Lorentz and gauge invariant  $ZV\gamma$  vertex is also in this case described by eight coupling parameters,  $h_i^V$ , ( $i = 1..4$ ) [23], where  $V = Z, \gamma$ . Combinations of the  $\mathcal{CP}$ -conserving ( $\mathcal{CP}$ -violating) parameters  $h_3^V$  and  $h_4^V$  ( $h_1^V$  and  $h_2^V$ ) correspond to the electric (magnetic) dipole and magnetic (electric) quadrupole transition moments of the  $ZV\gamma$  vertex. In the standard model all the  $ZV\gamma$  couplings vanish at tree level. Partial wave unitarity of the general  $f\bar{f} \rightarrow Z\gamma$  process restricts the  $ZV\gamma$  couplings uniquely to their vanishing SM values at asymptotically high energies [24]. Therefore, the coupling parameters have to be modified by form-factors  $h_i^V = h_{i0}^V/(1 + \hat{s}/\Lambda^2)^n$ , where  $\hat{s}$  is the square of the invariant mass of the  $Z\gamma$  system and  $\Lambda$  is the form-factor scale. The energy dependence of the form factor is assumed to be  $n = 3$  for  $h_{1,3}^V$  and  $n = 4$  for  $h_{2,4}^V$  [25]. Such a choice yields the same asymptotic energy behavior for all the couplings.

$D\mathcal{O}$  has searched for  $W$ -boson pair production  $\bar{p}p \rightarrow WW + X \rightarrow \ell\ell'\nu\nu'$  [26]. The channels considered are  $ee$ ,  $e\mu$  and  $\mu\mu$ . The standard selection cuts for  $W$ -events have an overall efficiency for  $W$ -pair production of  $\approx 0.07$  and with an integrated luminosity of  $\mathcal{L} \approx 14 \text{ pb}^{-1}$   $N_{exp}^{WW} = 0.47 \pm 0.08$  are expected from standard model processes. The most significant background to this process is  $t\bar{t}$  production. Because of the additional two  $b$ -jets in  $t\bar{t}$  events, this background can be eliminated relatively easily by a cut on the hadronic activity in the event.  $D\mathcal{O}$  applies a cut on the  $p_T$  of the  $WW$ -system,  $E_T^{HAD} = |-(\vec{E}_T^{\ell_1} + \vec{E}_T^{\ell_2} + \vec{p}_T)|$ , which is required to be less than 40 GeV. This requirement rejects about 75% of the  $t\bar{t}$  background with an efficiency of 95% (see fig. 7a). The searches in the  $ee\nu\nu$ ,  $e\mu\nu\nu$  and  $\mu\mu\nu\nu$  channels yield one signal event with an anticipated background of  $0.56 \pm 0.13$  events. An upper limit on the  $W$ -pair production cross section of  $\sigma(WW) < 87 \text{ pb}^{-1}$  has been set at 95% CL. Since the cross section increases very rapidly when the couplings deviate from their standard model values, the measured 95% CL upper limit on the cross section can be used to set limits on anomalous couplings.

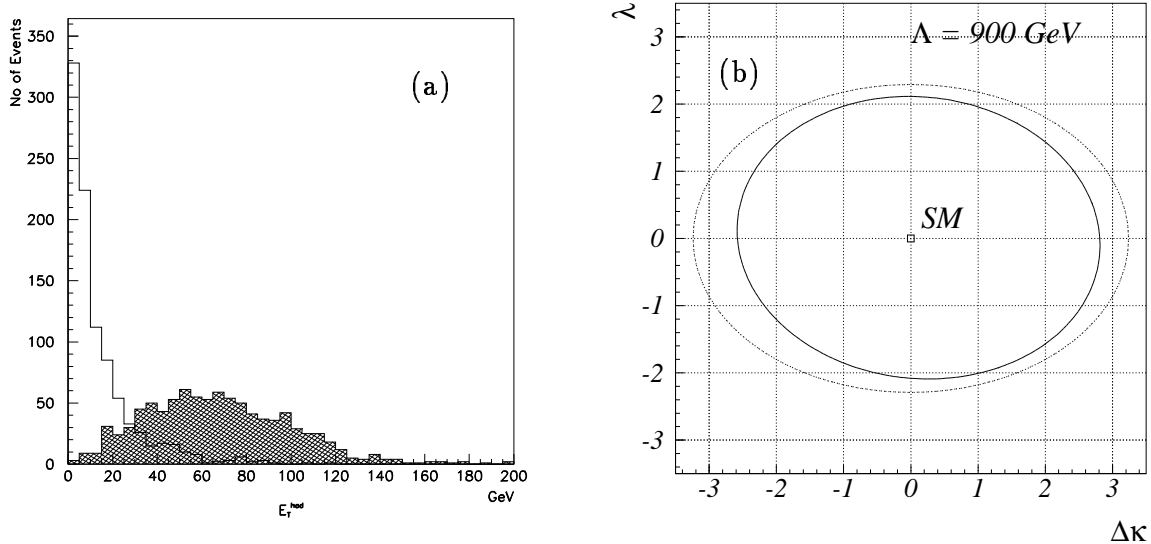


Figure 7: (a) Distribution of  $E_T^{HAD} = |-(\vec{E}_T^{\ell_1} + \vec{E}_T^{\ell_2} + \vec{\cancel{p}}_T)|$  for  $WW \rightarrow e\mu$  (histogram) and  $t\bar{t} \rightarrow e\mu$  events (hatched). (b) Contour limits on  $\Delta\kappa$  and  $\lambda$  from the measured  $WW \rightarrow \ell\ell'\nu\nu$  event rate.

plings. The limits on  $\Delta\kappa$  and  $\lambda$  are shown in figure 7b for a form factor scale of  $\Lambda = 900$  GeV. In general, limits on the couplings are quoted by varying only one independent coupling at a time, while keeping the other couplings fixed to their standard model value. The limits on  $\Delta\kappa$  and  $\lambda$  from this analysis are then  $-2.6 < \Delta\kappa < 2.8$  ( $\lambda = 0$ ) and  $-2.1 < \lambda < 2.1$  ( $\Delta\kappa = 0$ ), where  $\lambda_\gamma = \lambda_Z$  and  $\Delta\kappa_\gamma = \Delta\kappa_Z$  is assumed.

With large integrated luminosities it is possible to measure the  $W$ -pair production cross section. Based on an integrated luminosity of  $\mathcal{L} = 67$  pb $^{-1}$  CDF has done an analysis similar to the  $D\bar{D}$  analysis searching for  $W$ -pairs in the di-lepton channel using a jet veto, that is, events with jets with  $E_T(\text{uncorrected}) > 10$  GeV are rejected. The selection yields 5 signal events on a background of  $1.23 \pm 0.43$  events. The measured  $W$ -pair production cross section is  $\sigma(\bar{p}p \rightarrow WW) = (13.8_{-7.4}^{+9.2} \pm 2.9)$  pb, where the standard model predicts  $\sigma_{SM}(\bar{p}p \rightarrow WW) = (9.5 \pm 1.0)$  pb.

Searches for particle production requiring two leptons in the final state always suffer in rate because of the small leptonic branching ratios. Relaxing the requirements to a single lepton gives a substantial increase in event rate, though normally at the cost of a much larger background. CDF has looked for  $WW$  and  $WZ$ -production using hadronic decay channels [27]. The process  $\bar{p}p \rightarrow WW/WZ \rightarrow \ell\nu q\bar{q}'$  has been studied by selecting events with one high  $p_T$  lepton, large  $\cancel{E}_T$  and 2 jets with  $E_T > 30$  GeV. Since the jets come from the hadronic decay of the gauge boson, their invariant mass is required to be consistent with the gauge boson mass,  $60 < m_{jj} < 110$  GeV/ $c^2$ . Since no distinction can be made between  $WW$  and  $WZ$ -production in this selection, the sensitivity of the study was increased by including  $\bar{p}p \rightarrow WZ \rightarrow q\bar{q}'\ell\ell$  events, requiring the di-lepton invariant mass to reconstruct to the  $Z$ -boson mass.

The background from  $W/Z$ +jet production to these processes is about 30 times higher than for the signal production. Anomalous couplings, however, modify the differential distributions dramatically, especially the transverse momentum distribution of the  $W$ -boson. The ratio  $\frac{\sigma_{WW}(p_T^W=200 \text{ GeV})}{\sigma_{WW}(p_T^W=20 \text{ GeV})}$  is about  $10^{-3}$ , whereas for only modest deviations from the standard model couplings ( $\Delta\kappa = 0, \lambda = 1.0$ ) this ratio is about 0.5. By requiring a high  $p_T$  di-jet system,

$p_T(jj) > 130$  (100) GeV/c for the process  $\ell\nu jj$  ( $jj\ell\ell$ ) the background is completely eliminated and a very good sensitivity to anomalous couplings is retained. One completely loses sensitivity, however, to standard model  $WW/WZ$ -production. Figure 8a shows the  $m_{jj}$  distribution of the candidate events for  $WW/WZ \rightarrow \ell\nu jj$  after passing all selection cuts except the two-jet mass and two-jet  $p_T$  cuts. The  $p_T^{jj}$  spectrum of the events in the range  $60 < m_{jj} < 110$  GeV/c<sup>2</sup> is plotted in figure 8b. The dotted lines show the predicted standard model signal; the dashed lines are the predicted signal plus expected multi-jet and  $W/Z$ +jet backgrounds. One candidate event is observed with  $p_T^{jj} > 130$  GeV. No events passed all selection criteria for the di-lepton search.

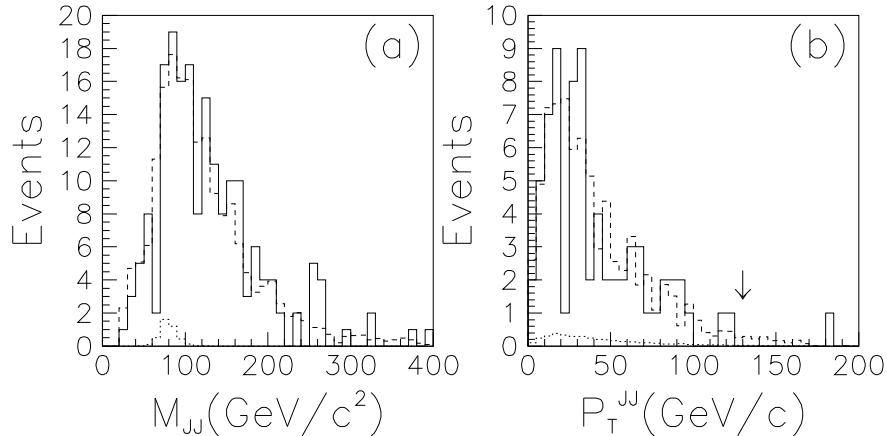


Figure 8: Selection of  $WW/WZ \rightarrow \ell\nu jj$  candidates. The  $m_{jj}$  distribution (a) of the events (solid line) passing all selection cuts except the two-jet mass and two-jet  $p_T$  cuts. The subset of events from (a) passing the two-jet mass cut is shown in (b). The dotted lines show the predicted standard model signal; the dashed lines are the predicted signal plus background distributions.

For standard model couplings 0.13 events are expected for  $WW/WZ \rightarrow \ell\nu jj$  and 0.02 events for  $WZ \rightarrow jj\ell\ell$ . Taking the observed one event as signal event, and comparing it with the rate expected for anomalous couplings, the limits on the anomalous couplings for a form factor  $\Lambda = 1000$  GeV are  $-1.11 < \Delta\kappa < 1.27$  ( $\lambda = 0$ ) and  $-0.81 < \lambda < 0.84$  ( $\Delta\kappa = 0$ ), where again  $\lambda_\gamma = \lambda_Z$  and  $\Delta\kappa_\gamma = \Delta\kappa_Z$  is assumed. If this restriction is relaxed and limits on  $\lambda_\gamma$  and  $\lambda_Z$  are derived, the constraint on  $\lambda_Z$  is about a factor 2 tighter because  $g_{WWZ}/g_{WW\gamma} = \cot\vartheta_w \approx 1.8$ .

The study of the production of photons in association with a  $W$  also permits a study of the  $WW\gamma$ -vertex [28, 29]. Most photons produced in association with a  $W$  are from initial or final state radiation, but the  $s$ -channel contribution of a photon radiated from a  $W$  directly probes the tri-gauge boson vertex.  $W\gamma$  events are selected by requiring, in addition to the regular  $W$  selection criteria, an isolated photon with transverse energy  $E_T^\gamma > 7$  (10) GeV for CDF ( $D\emptyset$ ). Photons are detected in the pseudo-rapidity range  $|\eta_\gamma| < 1.1$  for CDF and  $|\eta_\gamma| < 1.1$  or  $1.5 < |\eta_\gamma| < 2.5$  for  $D\emptyset$ . The photon identification efficiencies are approximately 80% for CDF and 75% (58%) for  $D\emptyset$  for the central (end) region. To reduce the contribution from radiative events the photon is required to be well separated from the lepton from the  $W$ -decay,  $\Delta R(\ell\gamma) > 0.7$ .

The number of signal events, after background subtraction, and the number of expected events from standard model processes are listed in table 4 for the electron and muon channels separately. Figures 9a and b show the distribution of the transverse cluster mass and photon  $p_T$ -spectrum for the CDF and  $D\emptyset$  data, respectively. The transverse cluster mass, defined as

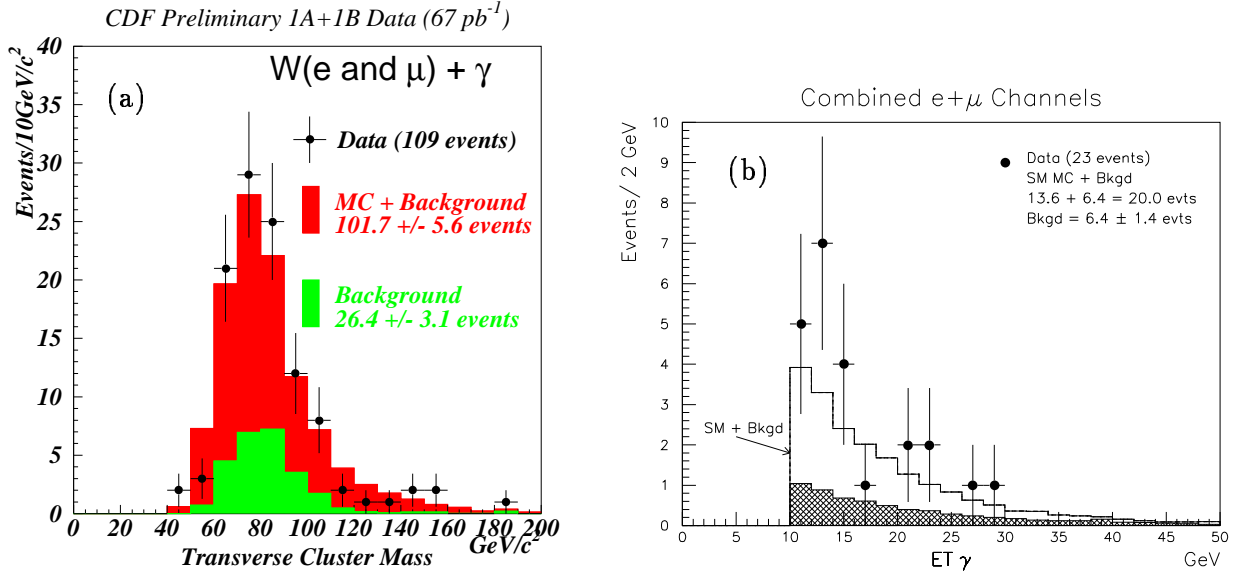


Figure 9: Distribution of the (a) transverse cluster mass and (b) photon transverse momentum spectrum for the CDF and DØ data.

$M_{CT}^2 = [(M_{\ell\gamma}^2 + |\vec{p}_T^\gamma + \vec{p}_T^\ell|^2)^{\frac{1}{2}} + p_T^\nu]^2 - |\vec{p}_T^\gamma + \vec{p}_T^\ell + \vec{p}_T^\nu|^2$ , is the minimum 3-body invariant mass of the lepton, photon and neutrino. Radiative events tend to populate the lower end of the  $M_{CT}$  and  $p_T^\gamma$  distribution;  $W\gamma$ -production events populate the high end of these distributions. Good agreement with the standard model predictions is observed.

In general, if the event statistics allows it, better limits on anomalous couplings are obtained by performing a maximum likelihood fit to a differential distribution rather than from the event rate. For  $W\gamma$  (and  $Z\gamma$ ) production a binned maximum likelihood fit is performed to the  $E_T^\gamma$ -spectrum as a function of the coupling constants. The last data bin is explicitly taken to be a zero-event bin. The limits thus obtained for a form-factor scale of  $\Lambda = 1.5$  TeV are  $-1.6 < \Delta\kappa < 1.8$  ( $\lambda = 0$ ) and  $-0.6 < \lambda < 0.6$  ( $\Delta\kappa = 0$ ), for DØ based on  $14 \text{ pb}^{-1}$  [29]. The preliminary limits from CDF are  $-1.8 < \Delta\kappa < 2.0$  ( $\lambda = 0$ ) and  $-0.7 < \lambda < 0.6$  ( $\Delta\kappa = 0$ ), based on  $67 \text{ pb}^{-1}$ . The DØ limits are slightly stronger, even though based on less integrated luminosity, because of the larger detector acceptance and because of the absence of very high  $p_T$  photons. The corresponding contours in  $\Delta\kappa$  and  $\lambda$  are shown in figure 10a. A vanishing magnetic dipole moment and electric quadrupole moment of the  $W$ , corresponding to  $\Delta\kappa = -\frac{1}{2}$  and  $\lambda = -\frac{1}{2}$  is excluded at 99% CL.

The decay rate for  $b \rightarrow s\gamma$  can also be used to set limits on anomalous couplings since the process is sensitive to photon radiation  $\gamma$  off the  $W$ -boson in the penguin diagram. The branching ratio has been measured by CLEO to be  $B(b \rightarrow s\gamma) = (2.32 \pm 0.57 \pm 0.35) 10^{-4}$  [30]. The upper limit on this branching ratio excludes the outer regions in the  $(\Delta\kappa, \lambda)$ -plane in figure 10a. The narrow region between the two allowed CLEO bands is excluded by the lower limit.

The study of  $Z\gamma$  anomalous couplings follows the same lines as the  $W\gamma$  analysis [31, 32]. Table 4 lists the expected and observed number of signal events for both experiments. The preliminary CDF limits on the anomalous couplings for a scale factor  $\Lambda = 500$  GeV, obtained from a likelihood fit to the  $p_T^\gamma$ -spectrum, are  $-1.6 < h_{30}^Z < 1.6$  ( $h_{40}^Z = 0$ ) and  $-0.4 < h_{40}^Z < 0.4$

	DØ 14 pb <sup>-1</sup>		CDF 67 pb <sup>-1</sup>	
	$W\gamma \rightarrow e\nu\gamma$	$W\gamma \rightarrow \mu\nu\gamma$	$W\gamma \rightarrow e\nu\gamma$	$W\gamma \rightarrow \mu\nu\gamma$
Signal	$9.0^{+4.2}_{-3.1} \pm 0.9$	$7.6^{+4.4}_{-3.2} \pm 1.1$	$58.9 \pm 9.0 \pm 2.6$	$23.7 \pm 5.9 \pm 1.1$
SM	$6.9 \pm 1.0$	$6.7 \pm 1.2$	$53.5 \pm 6.8$	$21.8 \pm 4.3$
	$Z\gamma \rightarrow ee\gamma$		$Z\gamma \rightarrow \mu\mu\gamma$	
	$Z\gamma \rightarrow ee\gamma$	$Z\gamma \rightarrow \mu\mu\gamma$	$Z\gamma \rightarrow ee\gamma$	$Z\gamma \rightarrow \mu\mu\gamma$
Signal	$3.6^{+3.1}_{-1.9}$	$1.9^{+2.6}_{-1.3}$	$17.1 \pm 5.7$	$12.5 \pm 3.6$
SM	$2.8 \pm 0.4$	$2.3 \pm 0.4$	$16.2 \pm 1.8$	$8.7 \pm 0.7$

Table 4: Number of signal and expected events for standard model couplings (SM) for  $W\gamma$  and  $Z\gamma$  production.

( $h_{30}^Z = 0$ ) for 67 pb<sup>-1</sup> of data. The corresponding DØ limits, based on 14 pb<sup>-1</sup>, are  $-1.9 < h_{30}^Z < 1.8$  ( $h_{40}^Z = 0$ ) and  $-0.5 < h_{40}^Z < 0.5$  ( $h_{30}^Z = 0$ ) [32]. Figure 10b summarizes all limits on  $h_{30}^Z, h_{40}^Z$ , including the preliminary result from the L3 experiment [33]. Its contour has a different orientation because of the different subprocess center of mass energy at which the events are produced in the  $e^+e^-$ -collisions.

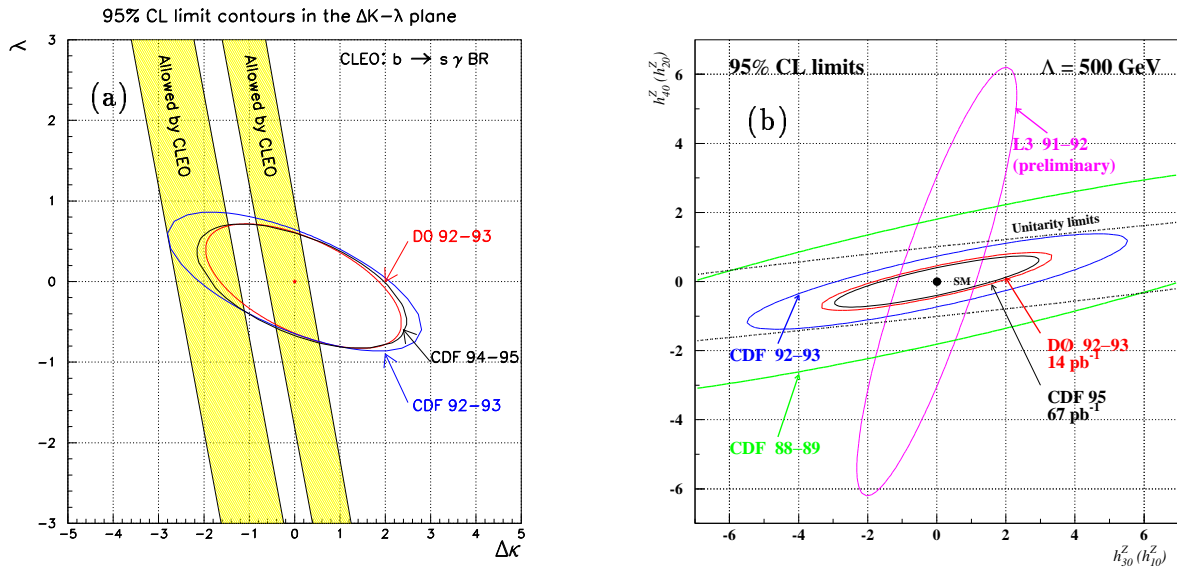


Figure 10: Limits on anomalous couplings (a)  $\Delta\kappa, \lambda$  from  $W\gamma$ -production from CDF, DØ and CLEO and (b)  $h_{30}^Z, h_{40}^Z$  from  $Z\gamma$ -production from CDF, DØ and L3.

## 6 Conclusions

A wide variety of properties of the  $W$  and  $Z$ -bosons are now being studied at hadron colliders with ever increasing precision. The mass of the  $W$ -boson is now measured to about two parts

per thousand. The magnetic moment of the  $W$  and its self-interactions are being probed and all results so far appear to be in good agreement with the standard model. With the large integrated luminosities collected by both the CDF and DØ experiment all measurements should benefit greatly from the new data.

## 7 Acknowledgements

I would like to thank my CDF and DØ colleagues, especially Hiro Aihara, Young-Kee Kim, Larry Nodulman and Tony Spadafora who have been most cooperative.

## References

- [1] S. Abachi *et al.* (DØ Collaboration), Nucl. Instr. Meth. **A338**, 185 (1994); H. Aihara *et al.* (DØ Collaboration), Nucl. Instr. Meth. **A325**, 393 (1993); S. Abachi *et al.* (DØ Collaboration), Nucl. Instr. Meth. **A324**, 53 (1993).
- [2] F. Abe, *et al.* (CDF Collaboration), Nucl. Instr. Meth. **A271**, 387 (1988).
- [3] F. Abe, *et al.* (CDF Collaboration), Phys. Rev. Lett. **73**, 220 (1994);  
F. Abe *et al.* (CDF Collaboration), Phys. Rev. **D52**, 2624 (1995).
- [4] W. F. Badgett in Proceedings of the 8th DPF Meeting, August 2-6 (1994), 431, Albuquerque, New Mexico  
F. Abe, *et al.* (CDF Collaboration), FERMILAB-PUB-95-301-E (1995) (submitted to Phys. Rev. Lett.)
- [5] S. Abachi *et al.* (DØ Collaboration), Phys. Rev. Lett. **75**, 1456 (1995)
- [6] R. Hamberg, W. L. van Neerven and T. Matsuura, Nucl. Phys. **B359**, 343 (1991);  
W. L. van Neerven and E. B. Zijlstra, Nucl. Phys. **B382**, 11 (1992).
- [7] M. Demarteau *et al.* DØ Note 2115/CDF Note 2552, 1994 (unpublished).
- [8] Particle Data Group, L. Montanet *et al.*, Phys. Rev. **D50**, 1173 (1994).
- [9] H. L. Lai *et al.*, Phys. Rev. **D51**, 4763 (1995).
- [10] J. L. Rosner, M. P. Worah and T. Takeuchi, Phys. Rev. **D49**, 1363 (1994).
- [11] C. Albajar *et al.* (UA1 Collaboration), Phys. Lett. **B253**, 503 (1991).
- [12] J. Alitti *et al.* (UA2 Collaboration), Phys. Lett. **B276**, 365 (1992).
- [13] G. Lopez Castro *et al.* Los Alamos preprint server, hep-ph/9504351
- [14] F. Abe *et al.* (CDF Collaboration), Phys. Rev. Lett. **74**, 341 (1995).
- [15] CDF Collaboration (F. Abe *et al.*) Phys. Rev. Lett. **74**, 850 (1995)
- [16] W. Giele, E. Glover, D. A. Kosower, Nucl. Phys. **B403**, 663 (1993).
- [17] A. D. Martin, R. G. Roberts and W. J. Stirling, Phys. Lett. **B306**, 145 (1993); **B309**, 492(E) (1993).

- [18] A. D. Martin, R. G. Roberts and W. J. Stirling, Phys. Rev. **D50**, 6734 (1994)
- [19] M. Glück, E. Reya, A. Vogt Z. Phys. **C67**, 433 (1995)
- [20] F. Abe *et al.* (CDF Collaboration), Phys. Rev. Lett. **75** 11 (1995);  
F. Abe *et al.* (CDF Collaboration), FERMILAB-PUB-95-033-E (1995) (submitted to Phys. Rev. D )
- [21] K. Kim and Y-S. Tsai, Phys. Rev. D **7**, 3710 (1973).
- [22] U. Baur and E.L. Berger, Phys. Rev. D **41**, 1476 (1990).
- [23] K. Hagiwara *et al.*, Nucl. Phys. **B282**, 253 (1987).
- [24] K. Hagiwara and D. Zeppenfeld, Nucl. Phys. **B274**, 1 (1986);  
U. Baur and D. Zeppenfeld, Phys. Lett. **201B**, 383 (1988).
- [25] U. Baur and E.L. Berger, Phys. Rev. **D47**, 4889 (1993).
- [26] S. Abachi *et al.* (DØ Collaboration), Phys. Rev. Lett. **75**, 1023 (1995)
- [27] F. Abe *et al.* (CDF Collaboration), Phys. Rev. Lett. **75**, 1017 (1995)
- [28] F. Abe *et al.* (CDF Collaboration), Phys. Rev. Lett. **74**, 1936 (1995)
- [29] S. Abachi *et al.* (DØ Collaboration), Phys. Rev. Lett. **75**, 1034 (1995).
- [30] M.S. Alam *et al.* (CLEO Collaboration), Phys. Rev. Lett. **74**, 2885 (1995) 2885.
- [31] F. Abe *et al.* (CDF Collaboration), Phys. Rev. Lett. **74**, 1941 (1995)
- [32] S. Abachi *et al.* (DØ Collaboration), Phys. Rev. Lett. **75**, 1028 (1995)
- [33] J. Busenitz in Proceedings of the 8th DPF Meeting, August 2-6 (1994), 1202, Albuquerque, New Mexico